PROCEEDINGS B

royalsocietypublishing.org/journal/rspb

Research

Cite this article: Carrillo JD, Torres Jimenez MF, Urrea-Barreto FJ, Pino K, Cooper RB, Antonelli A, Bacon CD, Faurby S, Silvestro D. 2026 Decoupled diversity and disparity after faunistic turnover in caviomorph rodents. *Proc. R. Soc. B* **293**: 20252586.
https://doi.org/10.1098/rspb.2025.2586

Received: 8 October 2025
Accepted: 15 January 2026

Subject Category:
Palaeobiology

Subject Areas:
palaeontology, evolution

Keywords:
body mass, diversification, morphological evolution, Rodentia, South America

Author for correspondence:
Juan D. Carrillo
e-mail: juan.carrillo@mnhn.fr

Electronic supplementary material is available online at https://doi.org/10.6084/m9.figshare.c.8290857.

THE ROYAL SOCIETY PUBLISHING

Decoupled diversity and disparity after faunistic turnover in caviomorph rodents

Juan D. Carrillo[1,2], Maria Fernanda Torres Jimenez[3], Francisco J. Urrea-Barreto[4,5], Kateryn Pino[6,7], Rebecca B. Cooper[8,9], Alexandre Antonelli[10,11,12,13], Christine D. Bacon[11], Soren Faurby[11] and Daniele Silvestro[11,14,15]

[1]CR2P (CNRS, MNHN, Sorbonne Université), Département Origines et Évolution, Museum National d'Histoire Naturelle, Paris 75005, France
[2]Department of Biology, University of Fribourg, Fribourg 1700, Switzerland
[3]Zoology, Institute of Biosciences, Life Sciences Center, Vilnius University, Vilnius LT- 10257, Lithuania
[4]Museo Paleontológico Egidio Feruglio, Trelew 9100, Argentina
[5]Smithsonian Tropical Research Institute, Panama City, Panama
[6]Facultad de Medicina Veterinaria, Universidad San Sebastián, Concepción 4070386, Chile
[7]Museo de Historia Natural, Universidad Nacional de San Agustin de Arequipa, Arequipa, Peru
[8]Department of Biology, University of Oslo Natural History Museum, Oslo 0316, Norway
[9]Centre for Planetary Habitability, University of Oslo, Oslo 0318, Norway
[10]Royal Botanic Gardens Kew, Richmond, London TW9 3AE, UK
[11]Department of Biological and Environmental Sciences, University of Gothenburg, Gothenburg 40530, Sweden
[12]Wuhan Botanical Garden,, Chinese Academy of Sciences, Wuhan 430074, People's Republic of China
[13]Department of Biology, University of Oxford, Oxford OX1 3EL, UK
[14]Department of Biosystems Science and Engineering, ETH Zurich, Basel 4056, Switzerland
[15]Swiss Institute of Bioinformatics, Lausanne 1015, Switzerland

JDC, 0000-0003-2475-3341; MFTJ, 0000-0002-7177-4164; FJU-B, 0000-0003-0913-5721; AA, 0000-0003-1842-9297; CDB, 0000-0003-2341-2705; SF, 0000-0002-2974-2628; DS, 0000-0003-0100-0961

Caviomorph rodents diversified widely in the Americas. Within this group, the sister clades Octodontoidea (spiny rats and allies) and Chinchilloidea (chinchillas and allies) illustrate strikingly imbalanced evolution, with 195 extant species in the former and only six in the latter. Fossil evidence, however, documents greater past diversity and disparity in Chinchilloidea, including the largest known rodents. Here, we integrate data from extant and extinct species to investigate how evolutionary dynamics shaped these contrasting trajectories. Using a phylogenetic framework, we reconstructed patterns of body mass and craniodental evolution. The ancestral body mass was small, but Chinchilloidea expanded into a broader size range, showing significantly higher rates of body mass evolution than Octodontoidea. Subsequent Neogene and Quaternary extinctions erased much of this variation, reversing a ~30 million-year trend of greater body mass disparity. Craniodental disparity, however, followed a different trajectory: initially higher in Chinchilloidea, it later became greater in Octodontoidea after the Miocene. Importantly, craniodental disparity remained relatively stable in both clades despite major diversification and extinction events. These findings highlight the decoupling of taxonomic diversity, body mass and craniodental morphology, underscoring the complexity of evolutionary dynamics even for sister clades that evolved on the same continent.

1. Introduction

Understanding the relationship between species richness (hereafter diversity) and morphological variation (hereafter disparity) is a major question in macroevolution [1]. Evolutionary models make predictions of the relationship between diversity and disparity. In adaptive radiations, a rapid diversification

is accompanied by ecological and morphological differentiation [2], whereas in non-adaptive radiations, clades diversify with minimal ecological and/or morphological differentiation [3]. In addition, extinction events can shape the diversity–disparity relationship in different ways. When extinction events are selective towards certain morphologies, diversity loss is accompanied by a decrease in disparity, whereas in extinction events affecting random lineages, morphological disparity can be unaffected by diversity loss [4,5].

The complex interactions between diversity and disparity in evolutionary radiations and extinctions can vary at different spatial and temporal scales and across taxonomic groups. Studies on a range of different taxa have yielded contrasting results, with some finding patterns of diversity and disparity to be coupled [6,7] and others not [8–10]. The heterogeneous relationship between diversity and disparity may be explained by differences in the selectivity of extinction events [4,11], geographically mediated diversification and ecologically mediated phenotypic evolution [12].

Incorporating fossil information into the study of evolutionary radiations is key to understanding the diversity–disparity relationship, as it directly documents diversification dynamics and morphological evolution in deep time. Fossils can also reveal morphological traits absent from living taxa. The fossil record has served to clarify the relationship between diversity and disparity in the evolutionary radiations of several clades, resulting in the recognition of coupling and decoupling patterns, depending on the taxa examined [4,10,13]. While studies of diversity and disparity throughout the radiations of clades at different geographic scales are required to elucidate general patterns, an informative test of these inferred patterns lies in comparing sister clades. Studying the evolution of sister clades that radiated within the same region can reveal underlying processes by removing potential confounding effects such as differences in the age of clades and evolutionary pressures in different biogeographic settings. Here, we combine data from extinct and living species to study the diversity–disparity relationship of sister clades at a continental scale.

Sister clades can show striking imbalances in diversity [14,15], and empirical phylogenetic trees are more imbalanced than predicted by simple macroevolutionary models [15,16]. Simulations and empirical data suggest that tree imbalance could be driven by differences in age-dependent speciation, stochastic population-level processes and the appearance of key innovations [16–19]. Sister clades may also follow different patterns of morphological evolution [20], although the links between tree imbalance and asymmetries in disparity among sister clades are not well understood.

South American mammals evolved in relative isolation during most of the Cenozoic [21], and their rich fossil record shows that their diversification dynamics have been affected by climatic, geologic and biotic events. In particular, the Andean uplift, climatic and landscape changes such as the establishment of mega-wetlands in Amazonia during the Miocene (Pebas and Acre systems), marine incursions in north-western and southern South America, and the expansion of grasslands in southern South America in the late Neogene [22–26], probably all contributed to shaping mammalian diversity patterns in the continent. The 'splendid' isolation of South American mammals was punctuated by dispersal events [27]. These included two notable long-distance dispersals from Africa, bringing the ancestors of caviomorph rodents and New World primates to the South American continent [28,29]. Furthermore, during the Eocene–Oligocene transition, a land connection between South America and the Caribbean islands may have facilitated dispersals from the continent to the islands via the Greater Antilles and Aves Ridge (GAARlandia) [30,31]. Finally, during the late Neogene, the gradual closure of the Central American Seaway and establishment of the Isthmus of Panama resulted in a faunal exchange between South, Central and North America known as the Great American Biotic Interchange (GABI) [32].

(a) The study group

Caviomorpha is a diverse clade of rodents endemic to the Americas, including the Caribbean islands. Their rich fossil record provides valuable insight into evolutionary patterns [33]. First recorded in South America during the Late Eocene–Early Oligocene (~36–30 Ma), caviomorphs probably arrived by rafting from Africa [28,29,34]. They rapidly radiated across the continent, and by the Late Oligocene (~27–23 Ma), major extant lineages were already present [29,31,33]. With their extensive fossil record, high ecological diversity and wide morphological variation, caviomorphs provide an excellent system for investigating diversification and morphological evolution [33,35–38].

Caviomorphs show extraordinary body mass variation, including the largest living rodent, the capybara (~60 kg) and the extinct *Josephoartigasia monesi* (~480 kg) [39–41]. Body mass represents a key axis of morphological disparity [42,43] because it correlates with several ecological and physiological traits, including metabolism, population dynamics and range size ([42] and references therein). Similarly, craniodental morphology reflects dietary and locomotor adaptations in rodents [44,45] and has been used to study spatial and temporal patterns in several rodent clades [12,46,47]. We therefore use body mass and craniodental traits as proxies to explore morphological disparity through time in caviomorphs.

Extant caviomorphs are grouped into four well-supported clades: Cavioidea, Chinchilloidea, Erethizontoidea and Octodontoidea [31,35,48]. Octodontoidea (spiny rats, tuco-tucos, hutias and relatives) and Chinchilloidea (chinchillas, pacaranas and allies) are sister clades forming Octochinchilloi [49], which diverged early in the caviomorph radiation [31,33,35,48–50]. Octodontoidea has an abundant fossil record documenting its evolution and past diversity [51–53]. Today, it includes 195 species distributed throughout the Americas and the Caribbean [37,50,54,55]. The genus *Ctenomys* alone comprises 68 living species—about 35% of extant octodontoid diversity [55]. Octodontoidea exhibits extensive ecological and morphological variation, including arboreal, burrowing, terrestrial and semiaquatic forms with diverse diets [36,52], including large species such as Caribbean capromyids (~3 kg) and South American echimyids (~6.9 kg) [56]. Despite this ecological breadth, Octodontoidea shows a narrower range of body mass in comparison with other caviomorphs [35].

In contrast to high Octodontoidea diversity, Chinchilloidea currently includes only six species [37,55], but fossils reveal far greater past diversity and body size variation [33,57–59]. The clade encompassed small chinchillas (~400 g) to giant extinct forms reaching 150–480 kg [40,41,60,61]. It also included the extinct Heptaxodontidae—large Quaternary caviomorphs from the Caribbean islands [31,62–65] (but see [64,65] for alternative relationships of *Elasmodontomys*). Following Neogene and Quaternary extinctions, Chinchilloidea became species-poor, now represented only by the Amazonian pacarana (*Dinomys branickii*) and five Andean species [37].

Here, we combine data from extant and extinct species of Octodontoidea and Chinchilloidea and use phylogenetic comparative methods in conjunction with a deep learning method to assess how diversification dynamics have contributed to the current imbalance in species diversity and to investigate the relationship between these dynamics and patterns of body mass and craniodental evolution. We then use these results to assess the diversity–disparity relationship between sister clades at a continental scale.

2. Results

We produced a time-calibrated phylogenetic tree of living and extinct Octodontoidea and Chinchilloidea by utilizing both molecular and morphological data. The inferred relationships among extant species are well supported (bootstrap node support for the families and main clades >0.90; electronic supplementary materials, figures S1 and S2) and are consistent with previous studies on extant clades [48,54]. The time calibrated phylogenetic analysis indicates an Early Oligocene origin for crown Octodontoidea and Chinchilloidea, with an age of origin of 33.0 Ma (CI = 29.2–36.9 Ma) for crown Octodontoidea and 32.2 Ma (CI = 29.9–35.1 Ma) for crown Chinchilloidea (electronic supplementary material, figure S3). The age of the Octochinchilloi clade (Octodontoidea + Chinchilloidea) was obtained from an independent analysis of the fossil record using a Bayesian Brownian bridge (BBB) model [66] and indicated a Late Eocene origin, with a mean of 36.5 Ma (95% credible interval [CI] = 33.0–40.8 Ma) (electronic supplementary material, figure S4).

(a) Body mass and craniodental disparity through time

We determined body mass disparity through time by analysing the evolution of body mass of extinct and extant Octodontoidea and Chinchilloidea using phylogenetic comparative methods. The ancestral body mass of Octochinchilloi (Chinchilloidea + Octodontoidea) was small, with a mean estimate of ~221 g (CI = 103–464 g). Both clades had small body masses at their origin, but Chinchilloidea evolved a higher body mass range through time (figure 1A,B), reaching the highest body mass values (up to ~480 kg) in the Pliocene and Pleistocene (5.3–0.012 Ma) before decreasing towards the present (figure 1A,B; electronic supplementary material, figure S5A). By contrast, Octodontoidea body mass remained relatively stable throughout the Palaeogene and Neogene, reaching its widest range of body mass in the Late Pleistocene (figure 1; electronic supplementary material, figure S5).

The estimated rate of body mass evolution was about 1.9 times higher in Chinchilloidea compared with Octodontoidea (figure 1C; electronic supplementary material, figure S5B; table 1). We identified a positive trend towards higher body mass in Chinchilloidea (posterior probability = 0.97; table 1) but did not find evidence for a trend in Octodontoidea (figure 1D, table 1). The trend parameter in Chinchilloidea was significantly higher than in Octodontoidea (posterior probability = 0.98). We repeated the analyses under a model without trend to assess its impact on our estimates. Additionally, since mammals converge towards intermediate sizes on islands and small species like rodents might have more frequent cases of increasing body mass than their continental counterparts, we also conducted the analyses excluding all the species occurring on islands to evaluate whether the overall patterns of body mass evolution were driven by the effect of insular evolution (electronic supplementary material, figure S7). The results and overall patterns of body mass evolution were consistent across models without a trend parameter and in analyses excluding island species (figure 1, electronic supplementary materials, figures S5 and S7). Excluding island species revealed a stronger difference in evolutionary rates between Chinchilloidea and Octodontoidea, with rates in Chinchilloidea being about three times higher.

We analysed craniodental disparity in extinct and extant Octochinchilloi using the morphological matrix assembled for phylogenetic inference. Analyses were restricted to the 63 species (14 extant, 49 extinct) scored for morphological data, comprising 35 Octodontoidea (10 extant, 25 extinct) and 28 Chinchilloidea (4 extant, 24 extinct). Because unscored entries (missing '?' or inapplicable '–' characters) can affect morphospace placement and bias disparity estimates [67], we performed two sets of analyses: one including all characters and another excluding characters with inapplicable scores. The overall patterns were consistent between the two approaches (figure 2D, electronic supplementary materials, figures S9 and S10). Across all species, Octodontoidea exhibited significantly greater craniodental disparity than Chinchilloidea (electronic supplementary material, figure S10). With the full character matrix, the difference was highly significant (Wilcoxon rank-sum test: $W = 1786$, $p = 4.1 \times 10^{-15}$) and remained so when characters with inapplicable entries were excluded ($W = 2735$, $p = 3.1 \times 10^{-8}$). Temporal patterns reveal that Chinchilloidea had greater disparity during the Oligocene, but this trend reversed after the Miocene, with Octodontoidea maintaining higher disparity into the present (figure 3D, electronic supplementary material, figure S9).

In addition, we examined cranial morphospace occupation in extant species of the two clades (figure 2A–C). Extant Octodontoidea occupied a larger morphospace area than Chinchilloidea; however, after accounting for differences in species diversity through random subsampling, the two clades showed no significant difference in morphospace occupation (figure 2B,C). For Octodontoidea, the median morphospace area was 0.090 (95% CI: 0.073–0.115, bootstrap, 10 000 replicates) and the value for Chinchilloidea (0.086) fell within this interval, confirming the lack of statistical difference. Thus, despite its much

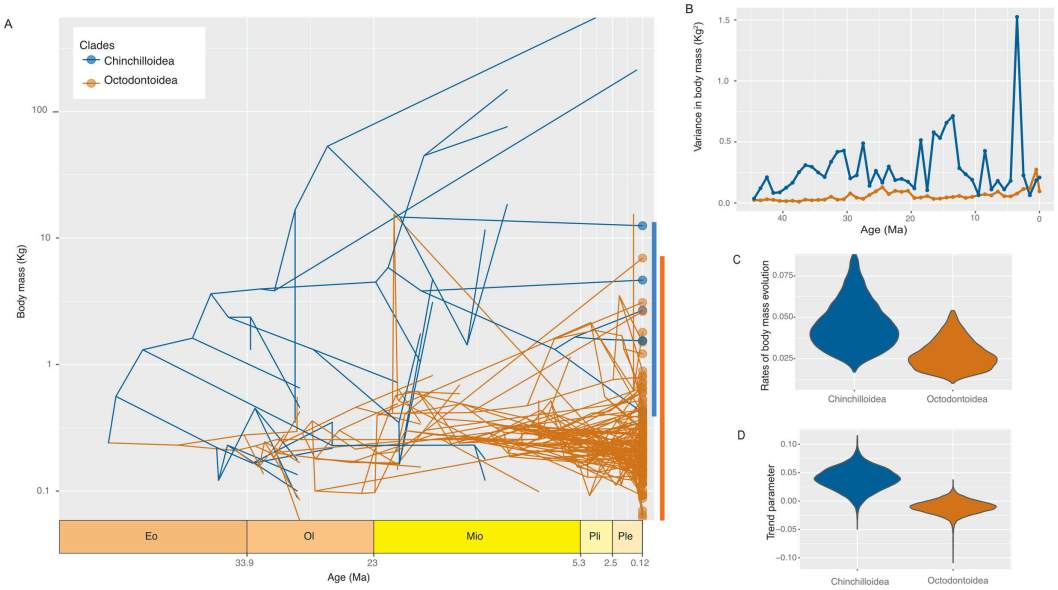

Figure 1. Diversification and body mass evolution in Octodontoidea and Chinchilloidea. (A) Phenogram of body mass evolution (log-transformed) for extinct and extant lineages, with ancestral states reconstructed under a fossilized Brownian motion model with trend across 100 phylogenetic trees (one shown). Lines show body mass trajectories through time, dots indicate extant species and coloured bars represent the extant body mass ranges of each clade. Both clades show similar ancestral body mass, but Chinchilloidea attained higher values through time, peaking in the Pliocene–Pleistocene before declining towards the present. Eo, Eocene; Ol, Oligocene; Mio, Miocene; Pli, Pliocene; Ple, Pleistocene. (B) Body mass disparity through time, estimated as variance within 1 Myr time bins, showing higher disparity in Chinchilloidea throughout most of the Palaeogene and Neogene, with lower values than Octodontoidea only after the Pliocene. (C) Violin plots of rates of body mass evolution, which are significantly higher in Chinchilloidea. (D) Violin plots of trend parameters, indicating support for a positive body mass trend in Chinchilloidea (>0), but not in Octodontoidea.

Table 1. Rates of body mass (BM) evolution in Octodontoidea and Chinchilloidea estimated with fossilized Brownian motion models with and without trend. Mean likelihoods and posterior probabilities of the trend parameter are shown. CI = credible interval.

no trend	**BM rates**				
	mean	**95% CI**			
Octodontoidea	0.0307	0.0119–0.0509			
Chinchilloidea	0.0521	0.0198–0.0935			
trend	**BM rates**		**trend parameter**		
	mean	95% CI	mean	95% CI	posterior probability
Octodontoidea	0.0299	0.0123–0.0504	−0.0108	−0.0335 to 0.0129	0.1731
Chinchilloidea	0.0484	0.0198–0.0843	0.0387	−0.0033 to 0.0750	0.968

lower extant diversity, Chinchilloidea occupies a substantial portion of the total cranial morphospace relative to Octodontoidea. Including body mass in the analysis did not alter the overall patterns (electronic supplementary material, figure S11).

(b) Diversity through time

We estimated diversity trajectories of Chinchilloidea and Octodontoidea to identify how and when the contemporary diversity imbalance unfolded. We used DeepDive software [68], which uses stochastic simulations to train deep learning models that predict diversity trajectories through time based on the spatiotemporal distribution of the fossil record. DeepDive models generate robust inferences of diversity through time from fossil occurrence data, while accounting for spatial, temporal and taxonomic variation in fossil sampling [68,69]. Training simulations were generated for many potential biodiversity curves and degraded to reflect the spatial and temporal properties of the empirical fossil record. The simulations used to train the model were able to capture the features of the empirical fossil occurrence data (electronic supplementary materials, figures S12 and S13) and the trained models had a low mean squared error (validation losses were 0.212 for Chinchilloidea and 0.164 for Octodontoidea).

The diversity trajectories of Chinchilloidea and Octodontoidea were initially similar, with a pattern of increasing diversity from their origin in the Eocene until the Early Oligocene, when a decrease in species diversity is observed in both clades (electronic supplementary material, figure S12). Subsequently, Octodontoidea diversity was higher until the Late Miocene (Tortonian: 11.6–7.3 Ma), at which point the two clades had similar diversity (figure 3). Until this point, the diversity trajectories of Octodontoidea and Chinchilloidea were similar, with a diversity increase during the Late Oligocene and subsequent decrease in the Middle Miocene (figure 3). After the Late Miocene, the two clades showed highly contrasting diversity trajectories.

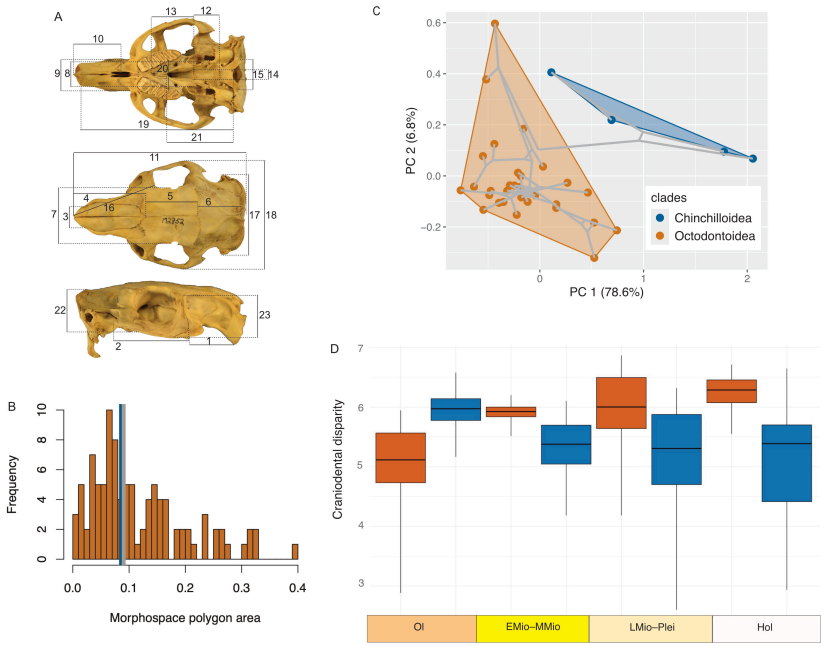

Figure 2. Craniodental disparity in Chinchilloidea (blue) and Octodontoidea (orange). (A) Cranial measurements used to estimate extant cranial morphospace, illustrated on the plains viscacha *Lagostomus maximus* (NMNH 172852) in ventral (top), dorsal (middle) and lateral (bottom) views; measurement numbers correspond to electronic supplementary material, table S1. (B) Frequency histogram of cranial morphospace occupation (convex hull area) for 100 random subsamples of five extant Octodontoidea species (matching sampled Chinchilloidea richness). The blue line indicates the Chinchilloidea morphospace area ($x = 0.086$) and the grey line the median of Octodontoidea subsamples ($x = 0.090$). (C) Cranial phylomorphospace of extant Chinchilloidea and Octodontoidea based on the first two principal components (PCs) from a principal components analysis (PCA) of cranial traits (33 octodontoids, 5 chinchilloids). The two viscacha species (*L. maximus* and *L. crassus*) overlap in morphospace. Despite lower species richness, Chinchilloidea occupies a substantial portion of the cranial morphospace. (D) Craniodental disparity through time, quantified as the sum of variances across PCAs from a taxon–character matrix excluding inapplicable characters, using MORD distances and arcsine square-root transformation. Boxplots show bootstrapped estimates (100 replicates). Ol, Oligocene; EMio–MMio, Early–Middle Miocene; LMio–Plei, Late Miocene–Pleistocene; Hol, Holocene.

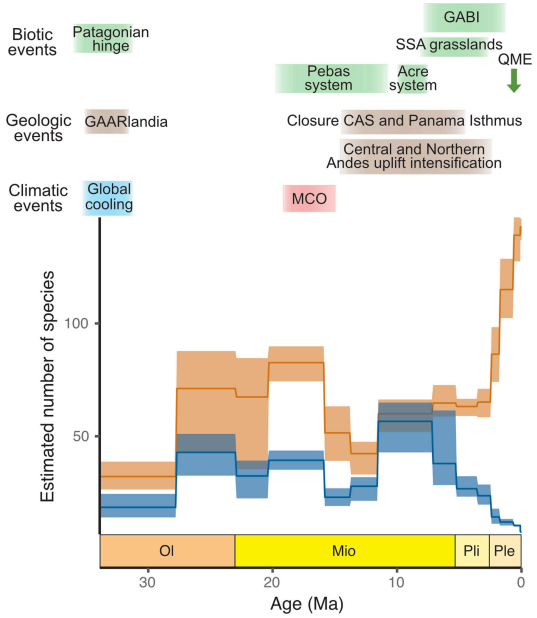

Figure 3. Species diversity dynamics of Chinchilloidea (blue) and Octodontoidea (orange) estimated with DeepDive [68]. Solid lines show mean species richness through time and shaded areas the 95% confidence intervals. Octodontoidea exhibits higher species diversity than Chinchilloidea for most of their evolutionary history. Both clades show similar diversity trajectories until the Late Miocene, after which Octodontoidea displays increasing diversity towards the present, whereas Chinchilloidea shows a sustained decline. Major climatic, geological and biotic events affecting South American mammal evolution since the Eocene–Oligocene transition are indicated at the top. Ol, Oligocene; Mio, Miocene; Pli, Pliocene; Ple, Pleistocene; CAS, Central American Seaway; MCO, Miocene Climatic Optimum; GAARlandia, Greater Antilles and Aves Ridge; GABI, Great American Biotic Interchange; SSA, Southern South America; QME, Quaternary Megafauna Extinction.

Octodontoidea showed a trend of increasing diversity from the Late Miocene until the present, whereas Chinchilloidea showed the opposite trend, with a diversity decrease from the Late Miocene until the present (figure 3). As a complementary analysis, we also used lineage through time (LTT) plots to quantify the diversity dynamics of the two clades (electronic supplementary material, figure S12). Although our phylogenetic dataset is not taxonomically exhaustive, it includes all living species (149) as

well as 52 extinct species and 40 extinct genera of Octochinchilloi, representing ~25% of the known extinct species diversity and ~30% of extinct generic diversity. The estimated diversity trajectories obtained using DeepDive and the LTT show qualitatively similar patterns (figure 3, electronic supplementary material, figure S12), with Chinchilloidea and Octodontoidea diverging in their diversity trajectories after the Middle Miocene.

3. Discussion

The mechanisms driving the coupling or decoupling of diversity and disparity remain unclear. Because disparity may correlate with clade age [12], comparing sister clades can account for this effect. If sister clades share similar environments within a continent, they are expected to show comparable diversity and disparity patterns under shared evolutionary pressures. However, our results reveal that two caviomorph sister clades followed contrasting evolutionary trajectories in South America. Integrating data from extant and extinct species, we show that differences in species diversity, body mass and craniodental morphology between these clades result from millions of years of divergence through a long history of heterogeneous morphological evolution alongside speciation and extinction dynamics.

Our analysis to estimate the age of origin of the Octochinchilloi clade (Octodontoidea + Chinchilloidea) from its present diversity and the fossil record using the BBB model [66] indicates that the clade originated in the Late Eocene (~36.5 Ma), shortly after the arrival of caviomorphs to South America. The oldest fossil records of caviomorphs on the continent are at least Early Oligocene in age [29], but possibly as old as the Eocene–Oligocene transition [28,34]. Fossils provide a minimum age, and our estimates of Late Eocene origin of Octochinchilloi agree with recent estimates of Middle Eocene origin of crown Caviomorpha [29].

As Octodontoidea and Chinchilloidea evolved on the same continent, they experienced similar geologic, climatic and biotic events during their evolutionary history. Nevertheless, we found that Chinchilloidea experienced higher rates of body mass evolution (posterior probability = 0.86), whereas Octodontoidea showed higher diversification rates, leading to the current imbalance in species diversity between the two clades. Despite its greater body mass disparity, Chinchilloidea generally maintained lower diversity than Octodontoidea across most of their evolutionary history. Extinctions during the late Neogene and Quaternary disproportionately reduced body mass disparity in Chinchilloidea. Patterns of craniodental disparity are more complex: Chinchilloidea showed higher disparity early in their evolutionary history during the Oligocene, but Octodontoidea showed higher craniodental disparity from that point onward. Unlike body mass disparity, craniodental disparity does not contrast as strongly with species diversity. We explore how diversification and body mass and craniodental disparity dynamics in both clades relate to major environmental and faunal changes in South America since the Eocene–Oligocene transition (figure 3).

(a) Diversity dynamics

The decline in diversity observed in both clades during the Early Oligocene (electronic supplementary material, figure S12) reflects the Patagonian Hinge, a faunal turnover in South American mammals driven by global cooling [22]. Following this event, Octodontoidea became more diverse than Chinchilloidea (figure 3). Octodontoidea diversity increased in the Late Oligocene during a diversification pulse in southern South America [53], declined in the Middle Miocene and then increased again in the Late Miocene, coinciding with the origin of most modern caviomorph lineages [53]. From the Late Miocene onwards, Octodontoidea diversity continued to increase steadily until the present (figure 3). Octodontoidea diversity surpassed Chinchilloidea during the Late Oligocene–Early Miocene and again from the Late Miocene to the present. The sharp contrast in extant species diversity between the two clades thus reflects their divergent diversification trajectories through the Neogene and Quaternary (figure 3).

The higher diversification rates of Octodontoidea are likely associated with significant environmental changes and geological events in South America, such as the central and northern Andean uplift during the Neogene [26]. For example, biogeographic studies based on phylogenies and geographic distribution of living species of spiny rats (Echimyidae, Octodontoidea) found that the lineage experienced dispersal and vicariant events among different biogeographic regions which contributed to elevated diversification rates [54,70]. The greater diversification of Octodontoidea may also be linked to their dispersal and subsequent radiation into other continental regions during the Neogene. Today, Octodontoidea occupies a much broader geographic range than Chinchilloidea [37], including lineages such as Echimyidae that colonized tropical Central America during the GABI [32,50]. In addition, biogeographical studies based on molecular data estimate that the hutias (Capromyidae, Octodontoidea) dispersed to the Caribbean islands during the Early to Middle Miocene [54,64], likely spurring additional diversification (figure 3).

The high modern octodontoid diversity is the result of steady diversification since the Late Miocene (figure 3). Approximately 35% of the total modern Octodontoidea diversity is represented by the 68 living tuco-tuco species (*Ctenomys*, Ctenomyidae) [55], which also exhibit the highest diversification rates within the clade [35]. The Ctenomyidae radiated since the Late Miocene–Early Pliocene (electronic supplementary material, figure S3) [35,50,53,71]. Extant *Ctenomys* have subterranean habits and occur in well-drained habitats in lowland and montane habitats of southern South America, and all species exhibit craniodental and anterior limb specializations for excavation [71,72]. The *Ctenomys* rapid diversification in the Plio-Pleistocene is probably related to increased aridity and the expansion of open biomes in southern South America [51]. The high *Ctenomys* diversity is an important component of the modern diversity imbalance between Octodontoidea and Chinchilloidea. However, our analyses showed that Octodontoidea have had higher diversity than Chinchilloidea since the Late Oligocene, predating the *Ctenomys* diversification.

The fossil record documents a higher diversity of Chinchilloidea in the past compared with their modern diversity of six species [33,59]. Chinchilloidea diversity remained relatively low in comparison with Octodontoidea (figure 2). After the diversity drop associated with the Patagonian Hinge (electronic supplementary material, figure S12), chinchilloid diversity stabilized, remaining relatively low until the Late Miocene, when the two clades showed similar diversity (figure 3). Subsequently, chinchilloid diversity steadily decreased until the present. The low diversification rates of Chinchilloidea during the Late Miocene and Pliocene reflect the extinction of lineages that reached gigantic sizes (>45 kg; [73]) within Dinomyidae and Neoepiblemidae [33,40,59]. Extinct giant dinomyids and neoepiblemids are recorded in Late Miocene and Pliocene sediments in both high (Ituzaingó Formation in Argentina, Camacho and San José Formations in Uruguay) and low (Solimões Formation in Brazilian Amazonia and Urumaco Formation in northwestern Venezuela) latitudes. Sedimentary evidence suggests that they inhabited estuarine or deltaic forested environments [33,41,57,60,74,75]. Some genera (e.g. *Phoberomys, Neoepiblema*) had a wide latitudinal distribution, occurring in southern and northern South America [57,59,74,75]. Based on sedimentary evidence and morpho-functional analyses, it has been proposed that *Phoberomys* and *Neoepiblema* inhabited water-related environments (e.g., rivers, wetlands) and were probably capable of swimming [58,60,61].

The causes of the extinction of giant dinomyids and neoepiblemids in South America remain uncertain. At higher latitudes, these clades may have been affected by increasing aridity, cooler climates and the expansion of grasslands during the Pliocene [33,75]. By contrast, the extinction drivers of tropical giant caviomorphs inhabiting water-related environments (e.g. *Phoberomys*, *Neoepiblema*) are still unknown. The uplift of the central and northern Andes, along with associated climatic and hydrographic changes, has been linked to the extinctions of aquatic vertebrates, such as crocodiles [76]. Future studies could test whether similar processes contributed to the loss of giant tropical rodents. Additional extinctions occurred in the Quaternary, including giant Chinchilloidea lineages, such as the Caribbean hutias, which probably disappeared owing to human activity [31,62,63,77]. Collectively, late Neogene and Quaternary extinctions drastically reduced Chinchilloidea diversity (figure 3), leaving only six extant species today [37].

(b) Body mass and craniodental evolution

The analysis of body mass evolution showed that the ancestral body mass of Octochinchilloi (Octodontoidea + Chinchilloidea) was small (~221 g, 95%CI = 103 – 463 g). Subsequently, Chinchilloidea evolved a high range of body masses in comparison with Octodontoidea, with a trend of increasing size through time, and some lineages reached giant sizes during the late Neogene and Quaternary (figure 1). Extant caviomorphs are characterized by large body mass ranges and high rates of body mass evolution [35]. Chinchilloidea is not the only caviomorph subclade that reached large sizes. The subclade Cavioidea also shows high rates of body mass evolution and includes the largest living rodent, the capybara, which can weigh ~50–60 kg [33,35].

Body mass increase in mammals is related to niche expansion, ecological specialization and reduced competition [43], among other possible factors, such as diet quality, digestive physiology, metabolism and climate [78–80]. The evolution of giant caviomorphs (e.g. capybaras (Hydrochoerinae) and chinchilloids (Neoepiblemidae and Dinomyidae)) from the Late Miocene to the Quaternary may have been influenced by niche expansion in response to changing environmental and climatic conditions, including the spread of open habitats and increased aridity in southern South America [33,35]. An increase in herbivore body mass is associated with the ability to feed on a wider range of plant parts and a decline in diet quality [78]. For example, the largest living rodent species, the capybara (*Hydrochoerus hydrochaeris*, Caviomorpha), is a hindgut fermenter with a highly efficient digestive system, and it is capable of feeding on low-nutritional vegetation during the dry season [39]. Within Chinchilloidea, large to giant sizes were also reached by the Caribbean giant hutias, representing an outstanding case of insular gigantism [62].

Octodontoid diversity has increased steadily since the Late Miocene (figure 3). However, this increase in diversity was not accompanied by high body mass differentiation, in comparison with Chinchilloidea (figure 1). Several living *Ctenomys* species have disjunct distributions, and molecular data indicate a rapid and early diversification in the *Ctenomys* radiation [72,81]. A similar pattern is seen in pocket gophers (Geomyidae), another group of burrowing rodents [82]. A scenario of rapid diversification with little overlap in distribution might explain the high diversification with minimal morphological modification.

Chinchilloidea showed high body mass disparity and relatively low diversity since early in its evolutionary history (figures 1 and 2). However, late Neogene and Quaternary extinctions drastically reduced its body mass disparity (figure 1A,B), leaving extant Chinchilloidea with much lower body mass variation today. These recent extinctions disproportionately impacted Chinchilloidea, reversing a pattern of relatively higher body mass disparity in comparison with Octodontoidea that appeared early in their evolutionary history (figure 1A).

The large body mass disparity of Chinchilloidea, despite its relatively low species diversity, may reflect the clade's tendency to evolve large sizes and the relatively high number of species that attained giant forms. Although not all species were large-bodied, many reached substantial sizes, contributing to the overall disparity. In living mammals, a negative relationship between species diversity and body mass has been proposed [83], although its magnitude might be overestimated owing to the recent megafauna extinctions. Such relatively low diversity among large-bodied mammals could be linked to broader range sizes, larger population requirements, longer generation times and reduced reproductive output [17,42,84], although disentangling the effects of these potential factors remains difficult.

Craniodental disparity shows different temporal patterns than body mass disparity. Chinchilloidea exhibited greater craniodental disparity than Octodontoidea during the Oligocene, but this pattern reversed after the Miocene (figure 2D). Unlike body mass disparity, craniodental disparity appears largely unassociated with diversification or extinction events, remaining

relatively stable in both clades since the Miocene (figure 2D). This pattern aligns with findings in extant South American cricetid rodents, in which cranial disparity is uncorrelated with diversification [9,85]. In this group, it has been suggested that higher rates of cranial morphological evolution occur in lineages with longer evolutionary histories, producing clades with fewer but more ecologically specialized species and, consequently, high morphological disparity [9]. More broadly, the decoupling of cranial disparity and species diversity in rodents may characterize continental radiations, where—unlike on islands—large geographic areas reduce spatial overlap among species, facilitating allopatric distributions of ecomorphological similar taxa [85]. In extant caviomorphs, cranial morphology exhibits a strong phylogenetic signal and is also associated with habitat [38]. Spatially explicit studies integrating (palaeo)environmental data with craniodental morphology in both extinct and extant caviomorphs would help clarify the drivers of craniodental morphological evolution in this group.

Our analysis of craniodental disparity based on a character matrix provides insights into its temporal dynamics (figure 2D). Discrete character matrices are valuable for studying patterns and rates of morphological evolution [67,86], but they also present methodological challenges, particularly for visualizing morphospace and handling missing data [67]. Missing or inapplicable characters can affect taxon placement in morphospace and bias disparity estimates [67]. Although our results remain robust when inapplicable characters are excluded (figure 2D, electronic supplementary material, figure S9), a high proportion of data is missing from the dataset (on average, 58% per species; electronic supplementary material, figure S8). Therefore, additional data would be useful to corroborate our findings about temporal patterns of craniodental disparity. Furthermore, when examining extant species using cranial measurements (figure 2A), we found that Chinchilloidea and Octodontoidea exhibit comparable levels of craniodental disparity once differences in species diversity are taken into account (figure 2B,C).

Overall, our results revealed contrasting patterns of diversity and disparity evolution for the sister clades Octodontoidea and Chinchilloidea. Extant octodontoid species diversity is 32-fold higher than the extant chinchilloid diversity. The dynamics that led to the modern diversity imbalance began in the Late Miocene and are attributed to higher diversification rates of Octodontoidea since the Late Miocene. By contrast, Chinchilloidea shows higher body mass disparity during the Neogene and Quaternary, including species that reached gigantic sizes. However, post-Pliocene extinctions in Chinchilloidea resulted in a substantial decline in body mass disparity within the group. Craniodental disparity, however, followed a different trajectory: initially higher in Chinchilloidea, it later became greater in Octodontoidea after the Miocene. Importantly, unlike body mass disparity, craniodental disparity appears largely unrelated to diversification and extinction dynamics, remaining relatively stable in both clades since the Miocene. Taken together, our results underscore the complexity of caviomorph evolutionary history and illustrate how diversity and disparity can follow decoupled trajectories even in closely related clades subject to similar environmental and biotic contexts.

4. Conclusion

Examining diversity imbalance and morphological evolution in sister clades unveils the relationship between taxonomic diversity and morphological disparity while controlling for clade age. Although one might expect sister clades that evolved under similar continental-scale climatic, geological and biotic conditions—and subject to comparable genetic constraints—to exhibit similar diversity and disparity patterns, our results show that this is not always the case. In caviomorph rodents, two sister clades that share a long evolutionary history in South America display markedly different diversification and morphological trajectories. We also show that extinction can disproportionately reduce disparity along specific axes (e.g. body mass), reversing evolutionary trends that persisted for millions of years, whereas its effects are largely unrelated to other axes (e.g. craniodental morphology). These findings highlight the complex and heterogeneous nature of evolutionary dynamics, illustrating how closely related clades that evolved on the same continent can nonetheless follow divergent evolutionary pathways.

5. Material and methods

(a) Time-calibrated phylogenetic analysis

We inferred a total evidence phylogenetic analysis by combining the molecular alignment with a morphological matrix of extinct and extant caviomorphs based on Boivin *et al*. [49] and Marivaux *et al*. [31]. For the morphological matrix, we included the Chinchilloidea and Octodontoidea species as scored in Marivaux *et al*. [31], plus the closely related *Mayomys* and *Eosallamys*. In addition, because of their relevance to analyses of trait evolution, we included the extinct species *Phoberomys pattersoni* and *J. monesi* that represent the largest body mass reached within Rodentia [40,41,60]. The modified morphological matrix is available in MorphoBank as Project 3402 (https://www.morphobank.org/permalink/?P3402).

We used the BBB model [66] to estimate the age of origin of the Octochinchilloi (Octodontoidea + Chinchilloidea) clade. The BBB model infers a clade's age of origin based on its present diversity and fossil record [66]. Then, we conducted a Bayesian time-calibrated phylogenetic analysis combining the molecular and morphological matrices using BEAST2 v. 2.6.7 [87]. The combined matrix includes 201 species (149 extant and 52 extinct) (electronic supplementary material).

(b) Body mass evolution analyses

We analysed body mass evolution in a phylogenetic framework using Bayesian inference as implemented in the fossilBM programme [80,88]. We acknowledge that body mass is only one of the many axes of morphological disparity and that it does not capture all the morphological variation in our study group. Nevertheless, body mass is the best-studied mammalian morphological trait and it correlates with several ecological and physiological traits [42]. Body mass can be estimated in extinct rodents from the fossil record [89], and it serves as a useful proxy for examining disparity dynamics in extinct and extant caviomorphs. We compiled body mass data for living species from the Phylacine database v. 1.2.1 [90] and additional published sources. Estimates for extinct species were gathered from the literature (electronic supplementary material, table S5) or calculated from dental measurements using the regression equations of Millien & Bovy [89] (electronic supplementary material, table S6). To analyse evolutionary dynamics, we applied the fossilBM Bayesian approach, which jointly estimates the rate and trend of trait evolution, as well as the ancestral states for all internal nodes. The rate and trend parameters can vary among clades [80] and as a function of time [88]. We used the fossilized Brownian motion model, both with and without trend, to evaluate the presence of positive or negative trends in the evolution of body mass (electronic supplementary material).

(c) Craniodental morphological variation

We analysed craniodental disparity in extinct and extant Octochinchilloi using the morphological matrix of 513 craniodental characters originally assembled for phylogenetic inference. From the 201 species in the full dataset, we excluded those represented only by molecular data. The final matrix contained 63 species (14 extant, 49 extinct), including 35 Octodontoidea (10 extant, 25 extinct) and 28 Chinchilloidea (4 extant, 24 extinct).

In our dataset, unscored entries (missing '?' or inapplicable '–' characters) were frequent, with a mean proportion of 58% per species (electronic supplementary material, figure S8). To evaluate the effect of missing data on the study of disparity patterns in Octochinchinlloi, we performed two analyses: one using the full set of 513 characters and another excluding all characters with at least one inapplicable entry, yielding a reduced matrix of 63 taxa and 118 characters. Analyses followed established analytical pipelines using the Claddis [86] and dispRity [91] packages (electronic supplementary material).

In addition, we constructed a phylomorphospace (i.e. the projection of a phylogenetic tree into a bivariate morphospace) using phytools [92]. We used the trait data (23 cranial measurements and body mass) collected for 38 extant species of Octodontoidea and Chinchilloidea. We performed a principal components analysis based on a variance–covariance matrix of the $\log_{10}$-transformed data with the FactoMineR package [93]. Finally, we used the maximum credibility tree obtained from the total evidence analysis (electronic supplementary material, figure S3), pruned to include only the 38 extant species with trait data, and constructed a phylomorphospace of the two principal components with phytools [92].

Extant Chinchilloidea is species poor (six species, five represented in our trait sample) in comparison with extant Octodontoidea (196 species, 33 represented in our trait sample) [55]. To account for differences in the number of extant species between the two clades, we resampled five Octodontoidea species at random from the trait dataset and calculated the area of the morphospace occupied (the area of the convex hull defined by those species). We resampled 100 times and calculated the frequency distribution and median of the morphospace area to compare with the area occupied by the five Chinchilloidea species.

(d) Inference of diversity dynamics

To evaluate the diversity dynamics through time of Chinchilloidea and Octodontoidea, we compiled the fossil occurrences of all the extinct species from the Paleobiology Database (paleobiodb.org/), the New and Old World database (nowdatabase.org/) and published literature (Dataset S5; electronic supplementary material) and analysed them using the DeepDive software [68]. DeepDive uses stochastic simulations of biodiversity and a deep learning model to infer diversity through time. Simulations showed that DeepDive is well-suited to estimate diversity dynamics at large spatial scales (e.g. continents), while accounting for spatiotemporal and taxonomic variation in fossil sampling [68,69]. Therefore, it is a suitable method to obtain robust inferences of palaeodiversity changes in Octodontoidea and Chinchilloidea in the Americas and the Caribbean. To inform the models about spatial biases in fossil sampling, we assigned each occurrence to one of the following bioregions: tropical lowlands, extra-tropical lowlands, Pampas-Chaco, central Andes and the Caribbean. We generated a configuration file through the DeepDiveR package [69], parameterizing the simulations and optimization of the deep learning model. The simulated datasets used for training were autotuned [69] to reflect the spatiotemporal distribution and total number of fossil occurrences in the empirical datasets. We trained two models, one for each clade, using two layers of long short-term memory units (LSTMs, 64 and 32 nodes) and two fully connected dense node layers (64 and 32 nodes). LSTMs are a type of recurrent neural network that accounts for the autocorrelated nature of time-series data, such as fossil data through time [68]. The models incorporated information on the number and temporal distribution of the observed occurrences, the number and duration of time bins (Cenozoic stages), spatial sampling biases and the current diversity of the two clades.

Ethics. This work did not require ethical approval from a human subject or animal welfare committee.

Data accessibility. All the input and output files of the analyses, as well as the associated code, are available in Dryad [94].

Supplementary material is available online [95]. The morphological matrix used in our study is available in MorphoBank as Project 3402.

Declaration of AI use. AI (ChatGPT, OpenAI, GPT-5 model) was used to assist with English language editing of the work. All scientific content, data interpretation and conclusions were developed solely by the authors.

Authors' contributions. J.D.C.: conceptualization, data curation, formal analysis, funding acquisition, investigation, methodology, project administration, resources, visualization, writing—original draft; M.F.T.J.: data curation, formal analysis, methodology, software, writing—review and editing; F.J.U.-B.: data curation, methodology, writing—review and editing; K.P.: data curation, formal analysis, methodology, writing—review and editing; R.B.C.: formal analysis, methodology, writing—review and editing; A.A.: conceptualization, funding acquisition, project administration, writing—review and editing; C.D.B.: conceptualization, funding acquisition, writing—review and editing; S.F.: conceptualization, funding acquisition, writing—review and editing; D.S.: conceptualization, formal analysis, funding acquisition, methodology, project administration, software, writing—review and editing.

All authors gave final approval for publication and agreed to be held accountable for the work performed therein.

Conflict of interest declaration. We declare we have no competing interests.

Funding. J.D.C. was supported by the Swiss National Science Foundation (SNSF) grants P2ZHP3_174749, P4P4PB_199187 and TMPFP2_209818, the Helge Ax:son Johnson Stiftelse grant F18-0486 and French National Research Agency grant ANR-24-ERCS-0007-01. D.S. received funding from ETH Zurich and the Swedish Foundation for Strategic Environmental Research MISTRA within the framework of the research programme BIOPATH (F 2022/1448). M.F.T.J. was supported by the European Union's Horizon Europe research and innovation programme under grant agreement No. 101130794 [ENTWINE]. R.B.C. was supported by the SNSF grant P500-3_235358. K.P. received funding from the British Ecological Society (Connecting Ecologists with Other Disciplines 2024 grant CE24/1004) and the WWF Russell E. Train Education for Nature program (EF 14066). A.A. was supported by the Swedish Research Council (2019-05191) and the Kew Foundation.

Acknowledgements. We would like to acknowledge the following curators for access to the collections under their care: D. Kalthoff (Naturhistoriska riksmuseet, Stockholm), M. Gelang (Naturhistoriska Museum, Gothenburg), V. Nicolas and A. Verguin (Museum National d'Histoire Naturelle, Paris), M. Surovy (American Museum of Natural History, New York), D. Lunde (National Museum of Natural History, Washington) and H. López (Instituto de Ciencias Naturales, Bogotá). We are grateful to R. Warnock and B. Allen for valuable comments. We thank two anonymous reviewers and the handling editor for their comments. The Interfaculty Bioinformatics Unit (IBU), University of Bern, provided computational infrastructure and support with bioinformatic analyses.

References

1. Benton MJ. 2015 Exploring macroevolution using modern and fossil data. *Proc. R. Soc. B* **282**, 20150569. (doi:10.1098/rspb.2015.0569)
2. Simpson GG. 1944 *The tempo and mode in evolution*. New York, NY: Columbia University Press.
3. Rundell RJ, Price TD. 2009 Adaptive radiation, nonadaptive radiation, ecological speciation and nonecological speciation. *Trends Ecol. Evol*. **24**, 394–399. (doi:10.1016/j.tree.2009.02.007)
4. Liu X, Song H, Chu D, Dai X, Wang F, Silvestro D. 2024 Heterogeneous selectivity and morphological evolution of marine clades during the Permian–Triassic mass extinction. *Nat. Ecol. Evol*. **8**, 1248–1258. (doi:10.1038/s41559-024-02438-0)
5. Foote M. 1993 Discordance and concordance between morphological and taxonomic diversity. *Paleobiology* **19**, 185–204. (doi:10.1017/s0094837300015864)
6. Harmon LJ, Schulte JA, Larson A, Losos JB. 2003 Tempo and mode of evolutionary radiation in iguanian lizards. *Science* **301**, 961–964. (doi:10.1126/science.1084786)
7. Rabosky DL, Santini F, Eastman J, Smith SA, Sidlauskas B, Chang J, Alfaro ME. 2013 Rates of speciation and morphological evolution are correlated across the largest vertebrate radiation. *Nat. Commun*. **4**, 1958. (doi:10.1038/ncomms2958)
8. Adams DC, Berns CM, Kozak KH, Wiens JJ. 2009 Are rates of species diversification correlated with rates of morphological evolution? *Proc. R. Soc. B* **276**, 2729–2738. (doi:10.1098/rspb.2009.0543)
9. Missagia RV, Casali DM, Patterson BD, Perini FA. 2023 Decoupled patterns of diversity and disparity characterize an ecologically specialized lineage of neotropical cricetids. *Evol. Biol*. **50**, 181–196. (doi:10.1007/s11692-022-09596-8)
10. Cantalapiedra JL, Prado JL, Hernández Fernández M, Alberdi MT. 2017 Decoupled ecomorphological evolution and diversification in Neogene-Quaternary horses. *Science* **355**, 627–630. (doi:10.1126/science.aag1772)
11. Pimiento C, Bacon CD, Silvestro D, Hendy A, Jaramillo C, Zizka A, Meyer X, Antonelli A. 2020 Selective extinction against redundant species buffers functional diversity. *Proc. R. Soc. B* **287**, 20201162. (doi:10.1098/rspb.2020.1162)
12. Zelditch ML, Li J, Tran LAP, Swiderski DL. 2015 Relationships of diversity, disparity, and their evolutionary rates in squirrels (Sciuridae). *Evolution* **69**, 1284–1300. (doi:10.1111/evo.12642)
13. Benson RBJ, Campione NE, Carrano MT, Mannion PD, Sullivan C, Upchurch P, Evans DC. 2014 Rates of dinosaur body mass evolution indicate 170 million years of sustained ecological innovation on the avian stem lineage. *PLoS Biol*. **12**, e1001853. (doi:10.1371/journal.pbio.1001853)
14. Mooers AO, Heard SB. 1997 Inferring evolutionary process from phylogenetic tree shape. *Q. Rev. Biol*. **72**, 31–54. (doi:10.1086/419657)
15. Henao-Diaz LF, Pennell M. 2023 The major features of macroevolution. *Syst. Biol.* **72**, 1188–1198. (doi:10.1093/sysbio/syad032)
16. Hagen O, Hartmann K, Steel M, Stadler T. 2015 Age-dependent speciation can explain the shape of empirical phylogenies. *Syst. Biol*. **64**, 432–440. (doi:10.1093/sysbio/syv001)
17. Valen LV. 1971 Adaptive zones and the orders of mammals. *Evolution (N Y)* **25**, 420–428. (doi:10.2307/2406935)
18. Hunter JP. 1998 Key innovations and the ecology of macroevolution. *Trends Ecol. Evol*. **13**, 31–36. (doi:10.1016/s0169-5347(97)01273-1)
19. Davies TJ, Allen AP, Borda-de-Água L, Regetz J, Melián CJ. 2011 Neutral biodiversity theory can explain the imbalance of phylogenetic trees but not the tempo of their diversification. *Evolution* **65**, 1841–1850. (doi:10.1111/j.1558-5646.2011.01265.x)
20. Blankers T, Townsend TM, Pepe K, Reeder TW, Wiens JJ. 2013 Contrasting global-scale evolutionary radiations: phylogeny, diversification, and morphological evolution in the major clades of iguanian lizards. *Biol. J. Linn. Soc*. **108**, 127–143. (doi:10.1111/j.1095-8312.2012.01988.x)
21. Simpson GG. 1980 *Splendid isolation. The curious history of south American mammals*. New Haven, CT and London, UK: Yale University Press.
22. Goin FJ, Abello MA, Chornogubsky L. 2010 Middle Tertiary marsupials from central Patagonia (early Oligocene of Gran Barranca): understaing South America's Grande Coupture. In *The Paleontology of Gran Barranca. Evolution and Environmental Change through the Middle Cenozoic of Patagonia* (eds RH Madden, AA Carlini, MG Vucetich, RF Kay), pp. 69–105. Cambridge, UK: Cambridge University Press.
23. Jaramillo C *et al*. 2017 Miocene flooding events of western Amazonia. *Sci. Adv.* **3**, e1601693. (doi:10.1126/sciadv.1601693)
24. Hoorn C *et al*. 2010 Amazonia through time: Andean uplift, climate change, landscape evolution, and biodiversity. *Science* **330**, 927–931. (doi:10.1126/science.1194585)

25. del Río CJ, Martínez SA, McArthur JM, Thirlwall MF, Pérez LM. 2018 Dating late Miocene marine incursions across Argentina and Uruguay with Sr-isotope stratigraphy. *J. South Am. Earth Sci*. **85**, 312–324. (doi:10.1016/j.jsames.2018.05.016)
26. Boschman LM. 2021 Andean mountain building since the Late Cretaceous: a paleoelevation reconstruction. *Earth Sci. Rev*. **220**, 103640. (doi:10.1016/j.earscirev.2021.103640)
27. Croft DA. 2012 Punctuated isolation. The making and mixing of South America's mammals. In *Bones, clones and biomes: the history and geography of recent neotropical mammals* (eds BD Patterson, LP Costa), pp. 9–19. Chicago, IL and London, UK: University of Chicago Press. (doi:10.7208/chicago/9780226649214.003.0002)
28. Antoine PO *et al*. 2012 Middle Eocene rodents from Peruvian Amazonia reveal the pattern and timing of caviomorph origins and biogeography. *Proc. R. Soc. B* **279**, 1319–1326. (doi:10.1098/rspb.2011.1732)
29. Campbell KE, O'Sullivan PB, Fleagle JG, de Vries D, Seiffert ER. 2021 An Early Oligocene age for the oldest known monkeys and rodents of South America. *Proc. Natl Acad. Sci. USA* **118**, e2105956118. (doi:10.1073/pnas.2105956118)
30. Iturralde-Vinent M. 1999 Paleogeography of the Caribbean region: implications for Cenozoic biogeography. *Bull. Am. Mus. Nat. Hist.* **238**, 1–95. (doi:10.2747/0020-6814.48.9.791)
31. Marivaux L *et al*. 2020 Early Oligocene chinchilloid caviomorphs from Puerto Rico and the initial rodent colonization of the West Indies. *Proc. R. Soc. B* **287**, 20192806. (doi:10.1098/rspb.2019.2806)
32. Carrillo JD, Faurby S, Silvestro D, Zizka A, Jaramillo C, Bacon CD, Antonelli A. 2020 Disproportionate extinction of South American mammals drove the asymmetry of the Great American Biotic Interchange. *Proc. Natl Acad. Sci. USA* **117**, 26281–26287. (doi:10.1073/pnas.2009397117)
33. Vucetich MG, Arnal M, Deschamps CM, Perez ME, Vieytes EC. 2015 A brief history of Caviomorph Rodents as Told by the Fossil Record. In *Biology of caviomorph rodents: diversity and evolution* (eds AI Vassallo, D Antenucci), pp. 11–62. Buenos Aires, Argentina: SAREM-Sociedad Argentina para el Estudio de los Mamíferos.
34. Antoine PO *et al*. 2021 Biotic community and landscape changes around the Eocene–Oligocene transition at Shapaja, Peruvian Amazonia: regional or global drivers? *Glob. Planet. Change* **202**, 103512. (doi:10.1016/j.gloplacha.2021.103512)
35. Álvarez A, Arévalo RLM, Verzi DH. 2017 Diversification patterns and size evolution in caviomorph rodents. *Biol. J. Linn. Soc*. **121**, 907–922. (doi:10.1093/biolinnean/blx026)
36. Ojeda RA, Novillo A, Ojeda AA. 2015 Large-scale richness patterns, biogeography and ecological diversification in caviomorph rodents. In *Biology of caviomorph rodents: diversity and evolution* (eds AI Vassallo, D Antenucci), pp. 121–138. Buenos Aires, Argentna: SAREM - Sociedad Argentina para el Estudio de los Mamíferos.
37. Maestri R, Patterson BD. 2016 Patterns of species richness and turnover for the South American rodent fauna. *PLoS One* **11**, 0151895. (doi:10.1371/journal.pone.0151895)
38. Álvarez A, Perez SI, Verzi DH. 2013 Ecological and phylogenetic dimensions of cranial shape diversification in South American caviomorph rodents (Rodentia: Hystricomorpha). *Biol. J. Linn. Soc.* **110**, 898–913. (doi:10.1111/bij.12164)
39. Herrera EA. 2013 Capybara digestive adaptations. In *Capybara: biology, use and conservation of an exceptional neotropical species* (eds JR Moreira, KMPMB Ferraz, EA Herrera, DW Macdonald), pp. 97–106. New York, NY: Springer. (doi:10.1007/978-1-4614-4000-0_5)
40. Engelman RK. 2022 Resizing the largest known extinct rodents (Caviomorpha: Dinomyidae, Neoepiblemidae) using occipital condyle width. *R. Soc. Open Sci*. **9**, 220370. (doi:10.1098/rsos.220370)
41. Rinderknecht A, Blanco RE. 2008 The largest fossil rodent. *Proc. R. Soc. B* **275**, 923–928. (doi:10.1098/rspb.2007.1645)
42. Lyons SK, Smith FA, Ernest SKM. 2019 Macroecological patterns of mammals across taxonomic, spatial, and temporal scales. *J. Mammal*. **100**, 1087–1104. (doi:10.1093/jmammal/gyy171)
43. Raia P, Carotenuto F, Passaro F, Fulgione D, Fortelius M. 2012 Ecological specialization in fossil mammals explains Cope's rule. *Am. Nat*. **179**, 328–337. (doi:10.1086/664081)
44. Verde Arregoitia LD, Fisher DO, Schweizer M. 2017 Morphology captures diet and locomotor types in rodents. *R. Soc. Open Sci.* **4**, 160957. (doi:10.1098/rsos.160957)
45. Samuels JX. 2009 Cranial morphology and dietary habits of rodents. *Zool. J. Linn. Soc*. **156**, 864–888. (doi:10.1111/j.1096-3642.2009.00502.x)
46. Wilson LAB, Sánchez-Villagra MR. 2010 Diversity trends and their ontogenetic basis: an exploration of allometric disparity in rodents. *Proc. R. Soc. B* **277**, 1227–1234. (doi:10.1098/rspb.2009.1958)
47. Gomes Rodrigues H, Lefebvre R, Fernández-Monescillo M, Mamani Quispe B, Billet G. 2017 Ontogenetic variations and structural adjustments in mammals evolving prolonged to continuous dental growth. *R. Soc. Open Sci*. **4**, 170494. (doi:10.1098/rsos.170494)
48. Upham NS, Patterson BD. 2015 Evolution of caviomorph rodents: a complete phylogeny and timetree for living genera. In *Biology of caviomorph rodents: diversity and evolution* (eds AI Vasallo, D Antenucci), pp. 63–120. Buenos Aires, Argentina: SAREM—Sociedad Argentina para el Estudio de los Mamíferos.
49. Boivin M, Marivaux L, Antoine PO. 2019 L'apport du registre paléogène d'Amazonie sur la diversification initiale des Caviomorpha (Hystricognathi, Rodentia): implications phylogénétiques, macroévolutives et paléobiogéographiques. *Geodiversitas* **41**, 143–245. (doi:10.5252/geodiversitas2019v41a4)
50. Upham NS, Patterson BD. 2012 Diversification and biogeography of the Neotropical caviomorph lineage Octodontoidea (Rodentia: Hystricognathi). *Mol. Phylogenetics Evol.* **63**, 417–429. (doi:10.1016/j.ympev.2012.01.020)
51. Verzi D, Olivares AI, Morgan CC. 2014 Phylogeny and evolutionary patterns of South American Octodontoid rodents. *Acta Palaeontol. Pol.* **59**, 757–769. (doi:10.4202/app.2012.0135)
52. Verzi DH, Olivares AI, Morgan CC, Álvarez A. 2016 Contrasting phylogenetic and diversity patterns in octodontoid rodents and a new definition of the family Abrocomidae. *J. Mamm. Evol.* **23**, 93–115. (doi:10.1007/s10914-015-9301-1)
53. Arnal M, Vucetich MG. 2015 Main radiation events in Pan-Octodontoidea (Rodentia, Caviomorpha). *Zool. J. Linn. Soc*. **175**, 587–606. (doi:10.1111/zoj.12288)
54. Fabre PH *et al*. 2017 Mitogenomic phylogeny, diversification, and biogeography of South American spiny rats. *Mol. Biol. Evol.* **34**, msw261. (doi:10.1093/molbev/msw261)
55. Mammal Diversity Database. 2022 Mammal Diversity Database. Zenodo. (doi:10.5281/zenodo.5945626)
56. Fabre PH, Vilstrup JT, Raghavan M, Sarkissian C, Willerslev E, Douzery EJP, Orlando L. 2014 Rodents of the Caribbean: origin and diversification of hutias unravelled by next-generation museomics. *Biol. Lett.* **10**, 20140266. (doi:10.1098/rsbl.2014.0266)
57. Carrillo JD, Sánchez-Villagra MR. 2015 Giant rodents from the Neotropics: diversity and dental variation of late Miocene neoepiblemid remains from Urumaco, Venezuela. *Palaontologische Zeitschrift* **89**, 1057–1071. (doi:10.1007/s12542-015-0267-3)
58. Kerber L, Candela AM, Ferreira JD, Pretto FA, Bubadué J, Negri FR. 2022 Postcranial morphology of the extinct rodent *Neoepiblema* (Rodentia: Chinchilloidea): insights into the paleobiology of neoepiblemids. *J. Mamm. Evol*. **29**, 207–235. (doi:10.1007/s10914-021-09567-4)
59. Rasia LL, Candela AM, Cañón C. 2021 Comprehensive total evidence phylogeny of chinchillids (Rodentia, Caviomorpha): cheek teeth anatomy and evolution. *J. Anat*. **239**, 405–423. (doi:10.1111/joa.13430)
60. Sánchez-Villagra MR, Aguilera OA, Horovitz I. 2003 The anatomy of the world's largest extinct rodent. *Science* **301**, 1708–1710. (doi:10.1126/science.1089332)
61. Geiger M, Wilson LAB, Costeur L, Sánchez R, Sánchez-Villagra MR. 2013 Diversity and body size in giant caviomorphs (Rodentia) from the northern Neotropics—a study of femoral variation. *J. Vertebr. Paleontol.* **33**, 1449–1456. (doi:10.1080/02724634.2013.780952)
62. Biknevicius AR, McFarlane D, Macphee RDE. 1993 Body size in *Amblyrhiza inundata* (Rodentia: Caviomorpha), an extinct megafaunal rodent from the Anguilla Bank, West Indies: estimates and implications. *Am. Mus. Novit* **3079**, 1–25. http://digitallibrary.amnh.org/dspace/handle/2246/4976

63. MacPhee RDE. 2011 Basicranial morphology and relationships of antillean Heptaxodontidae (Rodentia, Ctenohystrica, Caviomorpha). *Bull. Am. Mus. Nat. Hist*. **363**, 1–70. (doi:10.1206/0003-0090-363.1.1)
64. Woods R, Barnes I, Brace S, Turvey ST. 2021 Ancient DNA suggests single colonization and within-archipelago diversification of Caribbean caviomorph rodents. *Mol. Biol. Evol*. **38**, 84–95. (doi:10.1093/molbev/msaa189)
65. Da Cunha L *et al*. 2023 The inner ear of caviomorph rodents: phylogenetic implications and application to extinct West Indian taxa. *J. Mamm. Evol*. **30**, 1155–1176. (doi:10.1007/s10914-023-09675-3)
66. Silvestro D, Bacon CD, Ding W, Zhang Q, Donoghue PCJ, Antonelli A, Xing Y. 2021 Fossil data support a pre-Cretaceous origin of flowering plants. *Nat. Ecol. Evol.* **5**, 449–457. (doi:10.1038/s41559-020-01387-8)
67. Gerber S. 2019 Use and misuse of discrete character data for morphospace and disparity analyses. *Palaeontology* **62**, 305–319. (doi:10.1111/pala.12407)
68. Cooper RB, Flannery-Sutherland JT, Silvestro D. 2024 DeepDive: estimating global biodiversity patterns through time using deep learning. *Nat. Commun*. **15**, 4199. (doi:10.1038/s41467-024-48434-7)
69. Cooper RB, Allen BJ, Silvestro D. 2025 DeepDiveR – A software for deep learning estimation of palaeodiversity from fossil occurrences. *Meth. Ecol. Evol.* **16**, 1923–1934. (doi:10.1111/2041-210X.70070)
70. Upham NS, Ojala-Barbour R, Brito M J, Velazco PM, Patterson BD. 2013 Transitions between Andean and Amazonian centers of endemism in the radiation of some arboreal rodents. *BMC Evol. Biol*. **13**, 191. (doi:10.1186/1471-2148-13-191)
71. De Santi NA, Olivares AI, Piñero P, Villoldo JAF, Verzi DH. 2024 An exceptionally well-preserved fossil rodent of the South American subterranean clade *Ctenomys* (Rodentia, Ctenomyidae). Phylogeny and adaptive profile. *J. Mamm. Evol*. **31**, 35. (doi:10.1007/s10914-024-09732-5)
72. Castillo AH, Cortinas MN, Lessa EP. 2005 Rapid diversification of South American tuco-tucos (*Ctenomys*; Rodentia, Ctenomyidae): contrasting mitochondrial and nuclear intron sequences. *J. Mammal.* **86**, 170–179. (doi:10.1644/1545-1542(2005)086<0170:RDOSAT>2.0.CO;2)
73. Martin PS, Klein RG (eds). 1984 *Quaternary extinctions: a prehistoric revolution*. Buenos Aires, Argentina: University of Arizona Press.
74. Kerber L, Negri FR, Ribeiro AM, Nasif N, Souza-Filho JP, Ferigolo J. 2017 Tropical fossil caviomorph rodents from the southwestern Brazilian Amazonia in the context of the South American faunas: systematics, biochronology, and paleobiogeography. *J. Mamm. Evol*. **24**, 57–70. (doi:10.1007/s10914-016-9340-2)
75. Nasif NL, Candela AM, Rasia LL, Madozzo-Jaén MC, Bonini RA. 2013 Actualización del conocimiento de los roedores del Mioceno tardío de la Mesopotamia Argentina: aspectos sistemáticos, evolutivos y paleobiogeográficos. *El Neógeno de La Mesopotamia Argentina. Asociacion Paleontológica Argentina, Publicación Especial* **14**, 153–169.
76. Salas-Gismondi R, Flynn JJ, Baby P, Wesselingh FP, Antoine P, Salas-gismondi R. 2015 A Miocene hyperdiverse crocodylian community reveals peculiar trophic dynamics in proto-Amazonian mega-wetlands. *Proc. R Soc. B* **282**, 20142490. (doi:10.1098/rspb.2014.2490)
77. Turvey ST, Grady FV, Rye P. 2006 A new genus and species of 'giant hutia' (*Tainotherium valei*) from the quaternary of Puerto Rico: an extinct arboreal quadruped? *J. Zool*. **270**, 585–594. (doi:10.1111/j.1469-7998.2006.00170.x)
78. Clauss M, Steuer P, Müller DWH, Codron D, Hummel J. 2013 Herbivory and body size: allometries of diet quality and gastrointestinal physiology, and implications for herbivore ecology and dinosaur gigantism. *PLoS One* **8**, e68714. (doi:10.1371/journal.pone.0068714)
79. Clauss M, Dittmann MT, Müller DWH, Meloro C, Codron D. 2013 Bergmann's rule in mammals: a cross-species interspecific pattern. *Oikos* **122**, 1465–1472. (doi:10.1111/j.1600-0706.2013.00463.x)
80. Silvestro D *et al*. 2019 Early arrival and climatically-linked geographic expansion of new world monkeys from tiny African ancestors. *Syst. Biol*. **68**, 78–92. (doi:10.1093/sysbio/syy046)
81. Gardner SL. 2014 *New species of Ctenomys* Blainville *1826: (Rodentia: Ctenomyidae) from the lowlands and central valleys of Bolivia*. vol. **62**. Lubbock, TX: Museum of Texas Tech University. (doi:10.5962/bhl.title.142814)
82. Spradling TA, Brant SV, Hafner MS, Dickerson CJ. 2004 DNA data support a rapid radiation of pocket gopher genera (Rodentia: Geomyidae). *J. Mamm. Evol.* **11**, 105–125. (doi:10.1023/B:JOMM.0000041191.21293.98)
83. Gardezi T, da Silva J. 1999 Diversity in relation to body size in mammals: a comparative study. *Am. Nat.* **153**, 110. (doi:10.2307/2463899)
84. Damuth J. 1981 Population density and body size in mammals. *Nature* **290**, 699–700. (doi:10.1038/290699a0)
85. Maestri R, Monteiro LR, Fornel R, Upham NS, Patterson BD, de Freitas TRO. 2017 The ecology of a continental evolutionary radiation: Is the radiation of sigmodontine rodents adaptive? *Evolution* **71**, 610–632. (doi:10.1111/evo.13155)
86. Lloyd GT. 2016 Estimating morphological diversity and tempo with discrete character-taxon matrices: implementation, challenges, progress, and future directions. *Biol. J. Linn. Soc.* **118**, 131–151. (doi:10.1111/bij.12746)
87. Bouckaert R *et al*. 2019 BEAST 2.5: an advanced software platform for Bayesian evolutionary analysis. *PLOS Comput. Biol*. **15**, e1006650. (doi:10.1371/journal.pcbi.1006650)
88. Zhang Q, Ree RH, Salamin N, Xing Y, Silvestro D. 2022 Fossil-Informed Models Reveal a Boreotropical Origin and Divergent Evolutionary Trajectories in the Walnut Family (Juglandaceae). *Syst. Biol.* **71**, 242–258. (doi:10.1093/sysbio/syab030)
89. Millien V, Bovy H. 2010 When teeth and bones disagree: body mass estimation of a giant extinct rodent. *J. Mammal*. **91**, 11–18. (doi:10.1644/08-mamm-a-347r1.1)
90. Faurby S, Davis M, Pedersen RØ, Schowanek SD, Antonelli A, Svenning JC. 2018 PHYLACINE 1.2: The phylogenetic atlas of mammal macroecology. *Ecology* **99**, 2626–2626. (doi:10.1002/ecy.2443)
91. Guillerme T. 2018 dispRity: A modular R package for measuring disparity. *Methods Ecol. Evol*. **9**, 1755–1763. (doi:10.1111/2041-210x.13022)
92. Revell LJ. 2012 phytools: an R package for phylogenetic comparative biology (and other things). *Methods Ecol. Evol*. **3**, 217–223. (doi:10.1111/j.2041-210x.2011.00169.x)
93. Lê S, Josse J, Husson F. 2008 FactoMineR: an R package for multivariate analysis. *J. Stat. Softw* **25**, 1–18. (doi:10.18637/jss.v025.i01)
94. Carrillo JD, Torres Jiménez MFT, Urrea-Barreto FJ, Pino K, Cooper RB, Antonelli A, Bacon CD, Faurby S, Silvestro D. 2026 Data from: Decoupled diversity and disparity after faunistic turnover in caviomorph rodents. Dryad Digital Repository. (doi:10.5061/dryad.73n5tb3bc)
95. Carrillo JD, Torres Jiménez MF, Urrea-Barreto FJ, Pino K, Cooper RB, Antonelli A, Bacon CD, Faurby S, Silvestro D. 2026 Supplementary material from: Decoupled diversity and disparity after faunistic turnover in caviomorph rodents. Figshare. (doi:10.6084/m9.figshare.c.8290857)